

# 진동모드특성치를 이용한 철근콘크리트 구조물의 손상예측

## Damage Prediction in Reinforced Concrete Structures using Modal Response Parameters

김정태\*

Kim, Jeong-Tae

---

### 요 약

철근콘크리트 구조물의 손상을 진동반응특성치의 변화를 측정할 자료로부터 예측할 수 있는 실용적인 방법론이 제시되었다. 먼저, 구조물에 발생한 손상의 위치를 구조물 모드형상의 변화로부터 결정할 수 있는 알고리즘이 요약되었다. 다음으로, 실험크기 1/3 축소건조된 철근콘크리트 구조물을 사용한 실험에서 알고리즘을 이용하여 손상의 위치를 예측하였다. 이 실험과정에는 손상발생 전·후의 소수의 진동반응특성치가 사용되었다. 구조물의 손상을 예측한 결과로부터 알고리즘이 손상을 정확하게 발견하는 것으로 판명되었다.

### Abstract

A practical methodology to detect and localize damage in reinforced concrete structures by utilizing modal response parameters of as built and damaged states is presented. First, a damage detection algorithm which yields information on the location of damage directly from changes in mode shapes of structures is outlined. Next, the algorithm is implemented to detect and localize damage in a real, 1/3 scale, reinforced concrete structure. A set of pre-damage and post-damage modal parameters are used for the damage detection exercise. The results of the damage prediction show that the proposed algorithm can correctly locate the damage inflicted in the test structure.

**Keywords** : damage prediction, nondestructive, modal analysis, reinforced concrete structure, modal response parameters

---

\* 성회원, Research Associate, Department of Civil Engineering, Texas A&M University College Station, TX 77843-3136, USA

• 본 논문에 대한 토의를 1995년 2월 28일까지 학회로 보내 주시면 1995년 4월호에 토의회답을 게재하겠습니다.

## 1. INTRODUCTION

This paper deals with the general problem of utilizing changes in dynamic modal responses of structures to nondestructively detect, locate, and size damage in these structures. Structural damage may be defined as a deviation of a geometric and material property defining a structure that may cause unwanted displacements, distortions or vibrations in the structure. Many techniques of nondestructive damage evaluation are currently available to detect damage in structures. Such methods may include X-radiography, ultrasonics, eddy currents, thermography, neutron radiography, and acoustical holography. However, in many practical situations for large (and highly complex) civil engineering structures, the use of vibrational techniques to detect damage in large civil engineering structures may have several important advantages when compared to the techniques mentioned above. These advantages include the following: (1) the time period required to perform vibrational measurements can be short; (2) damage detection is not restricted to a local area; (3) damage can be detected from changes in modal response parameters (i.e., frequencies, mode shapes, and damping coefficients) measured by a few sensor readings.

During the past decade, a significant amount of research has been conducted in the area of damage detection using changes in modal responses. Research studies have related changes in frequencies to changes in beam properties such as cracks, notches or other geometrical changes (Gudmunson 1982; Chondros and Dimarogonas 1982). Other studies have also focused on the possibility of using the vibration characteristics of structures as an indication of structural damage (Cawley and Adams 1979;

O'Brien 1980; Kenley and Dodds 1980; Crohas and Lepert 1982). Recently, studies focusing on the vibrational approach to damage detection appear to be accelerating. Attempts have been made to monitor the structural integrity of bridges (Biswas et al. 1990; Flesch and Kernbichler 1990) and to investigate the feasibility of damage detection in aerospace structures using changes in modal parameters (Stubbs and Osegueda 1990; Chen and Garba 1988). Despite these combined research efforts, there are still outstanding needs: e.g., to detect, locate, and size damage in large (and highly complex) civil engineering structures for which only limited modal response parameters could be measured.

The objective of this paper is to present a practical methodology to detect the location of damage in reinforced concrete structures for which pre damage (i.e., as-built) and post-damage modal parameters are available for limited vibrational modes. The objective is met by the following tasks. Firstly, an algorithm to localize damage directly from changes in mode shapes of structures is formulated. Secondly, the algorithm is implemented to detect and localize damage in a 1/3 scale model of a reinforced concrete pier deck for which few lower resonant frequencies and mode shapes were monitored for as-built state and post-damage states.

## 2. DAMAGE LOCALIZATION ALGORITHM

The minimum design requirements for the damage localization algorithm to be described below include the following items: (1) the algorithm should accurately localize the damage; and (2) the algorithm should use a minimum set of mode shapes. The formulation here is restricted to the case when modal paramet-

ers of a prestine (undamaged) state and damaged states are available.

## 2.1 Theory

Consider a linear, undamaged, skeletal structure with NE elements and N nodes. The  $i^{\text{th}}$  modal stiffness,  $K_i$ , of the arbitrary structure is given by (Stubbs et al. 1992)

$$K_i = \Phi_i^T C \Phi_i \quad (1)$$

where  $\Phi_i$  is the  $i^{\text{th}}$  modal vector and C is the system stiffness matrix. The contribution of the  $j^{\text{th}}$  member to the  $i^{\text{th}}$  modal stiffness,  $K_{ij}$ , is given by

$$K_{ij} = \Phi_i^T C_j \Phi_i \quad (2)$$

where  $C_j$  is the contribution of the  $j^{\text{th}}$  member to the system stiffness matrix.

The fraction of modal energy for the  $i^{\text{th}}$  mode that is concentrated in the  $j^{\text{th}}$  member (i.e., the sensitivity of the  $j^{\text{th}}$  member to the  $i^{\text{th}}$  mode) is given by

$$F_{ij} = K_{ij} / K_i \quad (3)$$

Let the corresponding modal parameters in Eqs. 1 to 3 associated with a subsequently damaged structure be characterized by asterisks. Then for the damaged structure,

$$F_{ij}^* = K_{ij}^* / K_i^* = F_{ij} (1 + \sum_{k=1}^{NE} A_{ik} \alpha_k + \text{H.O.T.}) \quad (4)$$

where  $K_{ij}^*$  and  $K_i^*$  are given by, respectively,

$$K_{ij}^* = \Phi_i^{*T} C_j^* \Phi_i^*, \text{ and} \quad (5)$$

$$K_i^* = \Phi_i^{*T} C^* \Phi_i^* \quad (6)$$

where  $A_{ik}$  represents a set of coefficients associated with the mode  $i$  and location  $k$ ;  $\alpha_k$  is the fraction of damage at location  $k$  in the structure; and H.O.T. stands for higher order terms. On dividing Eq. 4 by Eq. 3, we obtain

$$\frac{F_{ij}^*}{F_{ij}} = \frac{K_{ij}^*}{K_{ij}} \frac{K_i}{K_i^*} \quad (7)$$

The quantities  $C_j$  and  $C_j^*$  in Eq. 2 and Eq. 5 may be written as follows:

$$C_j = E_j C_{j0}, \text{ and} \quad (8)$$

$$C_j^* = E_j^* C_{j0} \quad (9)$$

where the scalars  $E_j$  and  $E_j^*$ , respectively, are parameters representing the material stiffness properties of undamaged and damaged  $j^{\text{th}}$  member of the structure and the matrix  $C_{j0}$  involves only geometric quantities (and possibly terms containing Poisson's ratio).

On comparing Eqs. 4 and 7, we make the following observations: (1) for each location we can write an equation for each mode; (2) if the damage is to be specified in a small region, then we will have a large number of equations to define the system; and (3) we must find a way to determine the linear coefficients  $A_{ik}$  and the higher order terms. Before we proceed as suggested above, we pose the following question: Is there a way to utilize Eq. 7 without having to determine  $A_{ik}$  and solve a large system of linear or nonlinear equations?

To provide an answer to the question, we resort to the following simplification. We have observed from experiment results (e.g., Mazurek and DeWolf 1990) that the geometry of mode shapes in the vicinity of an undamaged element of a structure changes very little when the structure is damaged elsewhere. It has also been experimentally observed that rel-

ative modal deformations (i.e.,  $\Phi_i$ ) at a given location are larger after damage occurred (i.e., stiffness reduction occurs). From these observations and by assuming that the magnitude of damage in the structure is small, we further simplify Eq. 4 to the approximation that the modal strain energy ( $F_{ij}$ ) in an element remains the same before and after the damaging episode.

Consequently, we impose the approximation:

$$F_{ij} = F_{ij}^* \quad (10)$$

On substituting Eqs. 1, 2, 5, 6, 8 and 9 into Eq. 7; and rearranging, we obtain

$$\beta_{ji} = \frac{E_j}{E_j^*} = \frac{[\Phi_i^{*T} C_{j0} \Phi_i^*] K_j}{[\Phi_i^T C_{j0} \Phi_i] K_j^*} \quad (11)$$

in which the term  $\beta_{ji}$  is the damage localization indicator for the  $j^{\text{th}}$  member and the  $i^{\text{th}}$  mode. If we set  $K_j^* \approx \Phi_i^{*T} C_{j0} \Phi_i^*$ , all quantities on the right hand side (e.g.,  $\Phi_i$  and  $\Phi_i^*$ ) can be obtained or approximated from modal parameters derived from experimental measurements and the geometry ( $C_{j0}$ ) of the structure. Note that if higher order approximations (e.g., Eq. 4) are made to relate  $F_{ij}$  and  $F_{ij}^*$ , more complicated expressions result from which it may be difficult to isolate inflicted damage from measurable modal quantities.

From Eq. 11, damage is indicated at the  $j^{\text{th}}$  member and the  $i^{\text{th}}$  mode if  $\beta_{ji} > 1$ . To account for all available modes (NM) in the damage localization scheme, we form a single damage indicator for each location as

$$\beta_j = \frac{\sum_{i=1}^{NM} \{(\Phi_i^{*T} C_{j0} \Phi_i^*) K_j\}}{\sum_{i=1}^{NM} \{(\Phi_i^T C_{j0} \Phi_i) K_j^*\}} \quad (12)$$

Next we establish more robust classification

criteria for damage localization. For a given set of modes, the locations of damage are selected on the basis of a rejection of hypotheses in the statistical sense. Firstly, the value  $\beta_j$  ( $j=1,2,3,\dots,NE$ ) associated with each member is treated as a realization of a random variable  $\beta$ . In other words, the collection of the damage indices,  $\beta_j$ , represent a sample population. For purposes of making a consistent comparison, we wish to classify a location into one of two groups. We first normalize the values of the indicator  $\beta_j$  ( $j=1,2,3,\dots,NE$ ) according to the rule

$$Z_j = \frac{\beta_j - \bar{\beta}}{\sigma_\beta} \quad (13)$$

in which the terms  $\bar{\beta}$  and  $\sigma_\beta$  represent, respectively, the mean and the standard deviation of the collection of  $\beta_j$  values.

Our next problem is to develop an algorithm that would classify the  $Z_j$ s into damaged and undamaged locations. A solution to this problem can be obtained in several ways which include, but are not limited to, techniques from statistical hypothesis testing (Gibson and Melsa 1975), signal detection (Nielson 1991), and classification analysis (Kosko 1992). Here we classify the damage pattern via a statistical pattern recognition technique using hypothesis testing (Gibson and Melsa 1975).

The localization scheme used here constitutes essentially a detector which accepts a specific value of the damage index as input and provides as output a decision regarding the likelihood that the structure is damaged at that location. The null hypothesis is that the structure is not damaged at the  $j^{\text{th}}$  member (i.e.,  $H_0$ ). If  $H_0$  is true, we assume the distribution of the damage indices to be given by  $f_\beta(\beta/H_0)$ . The alternate hypothesis is that the structure

is damaged at the  $j^{\text{th}}$  member (i.e.,  $H_j$ ). For a given damage index  $\beta_j$ , the probability that the structure is not damaged at the  $j^{\text{th}}$  member when  $H_j$  is true is given by (Gibson and Melsa 1975):

$$P_j = 1 - \int_0^{\beta_j} f_{\beta}(\beta/H_0) d\beta \quad (14)$$

or the confidence that the  $j^{\text{th}}$  member is a damaged location is  $1 - P_j$ .

### 2.2 Experimental Verification

To check the feasibility of using the damage localization theory to detect and locate damage in structures, a group of verification tests have been performed on numerical examples as well as laboratory-controlled structures. The demonstrations of those tests are fully described in (Stubbs, Kim, and Topole 1992), (Stubbs, Kim, and Topole 1993), and (Kim and Stubbs 1994).

### 3. DAMAGE DETECTION IN A REINFORCED CONCRETE DECK

In this section, we demonstrate the practicality of the damage detection theory by locating damage in a real, reinforced concrete structure for which as-built and damaged modal parameters were measured for few vibrational modes. This objective is met in four steps: firstly, we describe the test structure; secondly, we describe the measured modal parameters of the test structure; thirdly, we develop a damage detection model of the test structure; and finally, we perform damage localization in the test structure.

### 3.1 Description of the Test Structure

The Naval Civil Engineering Laboratory (NCEL) performed laboratory experiments on a 1/3 scale model of a reinforced concrete pier deck to monitor changes in modal response parameters due to structural degradation (Eggers and Stubbs 1993). A schematic of the structure is shown in Fig. 1. The structure consists of 5-3/8 inch (13.7cm) thick, 31×18 square feet (9.5m×5.5m) area, flat slab supported by six equally spaced supports (which are rectangular pile caps spaced at 5 feet (1.5m)). The supports and deck form a monolithic system. Each of the five deck spans is reinforced along the x direction. Steel for temperature control is placed along the y-direction. The principal slab reinforcement consisted of No. 2 and No. 3, deformed, grade 60 bars used with 4,000 psi (27,600 kPa) concrete (designed compression strength). Reinforcing clear cover was 1 inch (2.54cm) on the bottom and 5/8 inch (1.58cm) on the top of the slab. The maximum aggregate size was 3/8 inch (0.95cm). The pier deck was cast in place and the measured modulus of elasticity for the spans was 4,000 ksi (27,600 kPa) with a Poisson's ratio of 0.15.

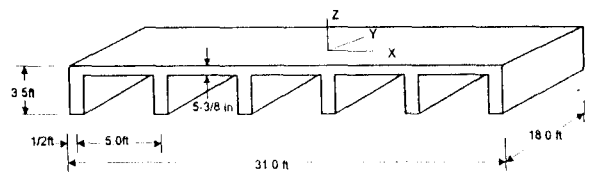


Fig. 1 Schematic of the 1/3-scale reinforced concrete deck

### 3.2 Description of Measured Modal Parameters of the Test Structure

As schematized in Fig. 2, the measurement of modal responses came with an accelerometer and a hammer kit, which was a 12 pound (54 N) sledge hammer to excite the different vibrational frequencies of the test structure. The hammer was capable of transferring the force into an electrical signal. The measured electrical signals from the impact forces and accelerations were converted and processed with a spectrum analyzer. The main function of the two-channel spectrum analyzer was to convert the analog signals from the hammer and accelerometer to a digital format and to transform the time domain data to frequency domain with the aid of the Fast Fourier Transform (FFT). Also, a filtering system (e.g., the SMS modal analysis package; see Star Reference Manual (1990)) produced the best possible Frequency Response Functions (FRFs).

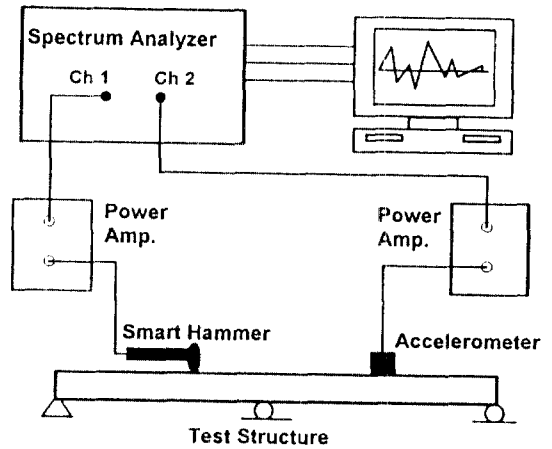


Fig. 2 Schematic of the modal response measurement

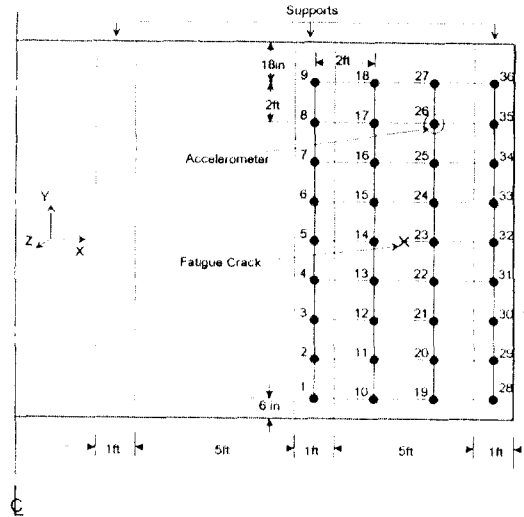
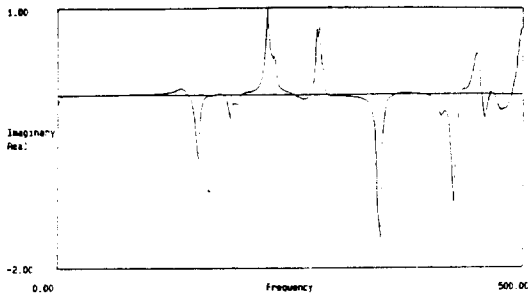


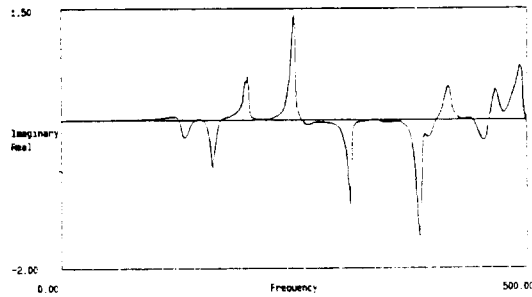
Fig. 3 Experimental arrangement on the reinforced concrete deck

The experimental arrangement used to measure modal responses of the structure is shown in Fig. 3. An accelerometer was placed at Node 26 and the excitation hammer was moved from Node 1 to Node 36. Two levels of damage were inflicted upon a location of the deck in the middle of two nodes Node 14 and Node 23. The first damage stage was simulated by fatigue crack tests using the following load cycles: (a) 0 to 10 kips (69 mPa) for 15 cycles, (b) 0 to 30 kips (207 mPa) for 15 cycles, (c) 0 to 60 kips (414 mPa) for 15 cycles, and (d) 0 to 90 kips (621 mPa) for 20 cycles. The second damage stage was simulated by the load to failure tests using the ultimate load of 110 kips (759 mPa). For each damage case, modal response data were measured in forms of FRFs. Furthermore, frequencies and mode shapes were extracted from the

FRFs by using the SMS modal analysis package. Fig. 4 illustrates FRF curves for the two damage cases of the structure. Figs. 5-7 shows three out-of-plane flexural modes of the structure. In each figure, mode shapes and frequencies for undamaged (as-built) state and two damaged states of the structure are identified.

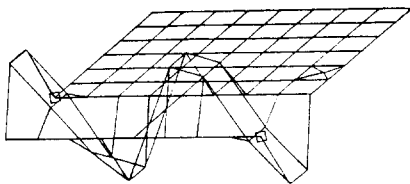


(a) First Damage Stage

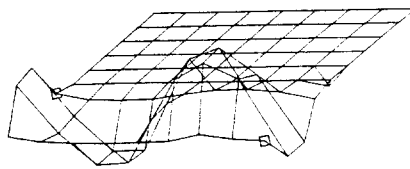


(b) Second Damage Stage

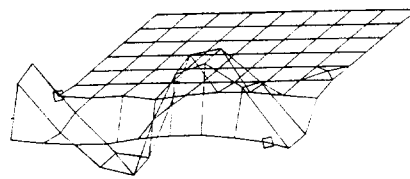
Fig. 4 Comparative shapes of FRFs for two damage states



(a) Undamaged State (174.49 Hz)

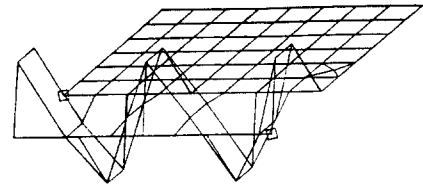


(b) Damage Stage One (165.90 Hz)

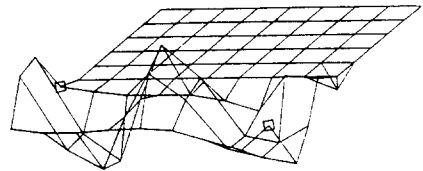


(c) Damage Stage Two (159.62 Hz)

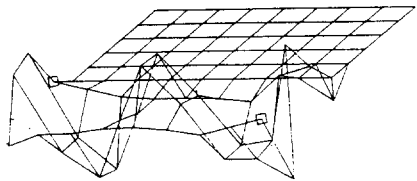
Fig. 5 Identification of first flexural mode



(a) Undamaged State (211.42 Hz)

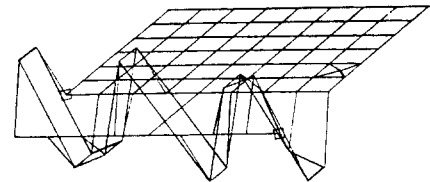


(b) Damage Stage One (198.87 Hz)

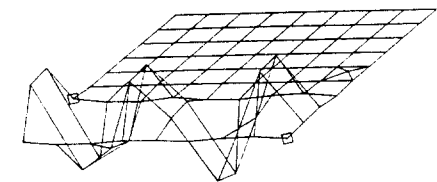


(c) Damage Stage Two (197.68 Hz)

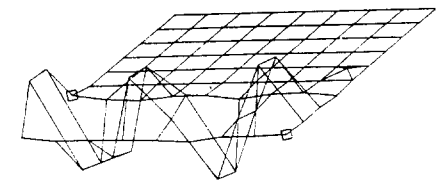
Fig. 6 Identification of second flexural mode



(a) Undamaged State (259.74 Hz)



(b) Damage Stage One (250.51 Hz)



(c) Damage Stage Two (230.98 Hz)

Fig. 7 Identification of third flexural mode

### 3.3 Damage Detection Model

As a damage detection model (i.e., a mathematical representation of a structure with degrees of freedom limited corresponding to sensor readings) of the test structure, we selected a grid model. A schematic of the grid model which consists of 43 grid beam elements is shown in Fig. 8. This damage detection model was selected on the basis of the following two reasons: first, the mode shapes of the structure provided modal information that could be utilized by a one or two-dimensional model such as a beam or a plate (note that the accelerometers mounted on the deck measured only vertical motion in z-direction); and second, the deck behaved essentially as a plate which can be modeled as a gridwork system.

For the grid model shown in Fig. 8, three degrees of freedom are permitted at each joint: a displacement in the z-direction, a rotation about the x-axis, and a rotation about the y-axis. The fraction of modal energy of member  $j$  and node  $i$  for the grid model is computed from an equivalent form of Eq. 3 (i.e.,  $F_{ij} = E_j[\Phi_i^T C_{j0} \Phi_i] / K_i$ ) as follows (See Ugural (1981) for details):

$$C_{j0} = \begin{bmatrix} \frac{12}{l^3} & \frac{6}{l^2} & \frac{-12}{l^3} & \frac{6}{l^2} \\ \frac{6}{l^2} & \frac{4}{l} & \frac{-6}{l^2} & \frac{2}{l} \\ \frac{-12}{l^3} & \frac{-6}{l^2} & \frac{12}{l^3} & \frac{-6}{l^2} \\ \frac{6}{l^2} & \frac{2}{l} & \frac{-6}{l^2} & \frac{4}{l} \end{bmatrix}_j$$

$$\Phi_i = \begin{bmatrix} \phi_{xa} \\ \phi_{ya} \\ \phi_{xb} \\ \phi_{yb} \end{bmatrix} \quad (15)$$

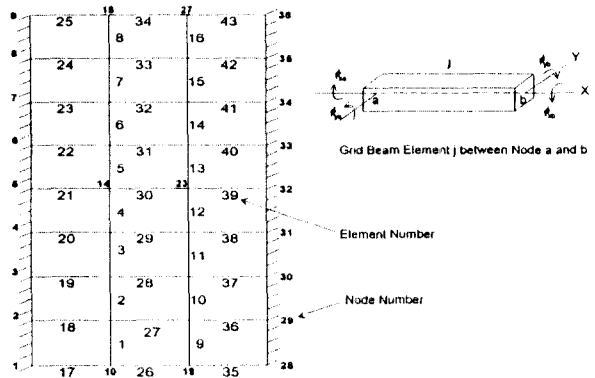


Fig. 8 Schematic of the damage detection model

where the four rotational degrees of freedom are defined as:  $\phi_{xa} = (\partial\phi(x,y)/\partial x)_a$ ,  $\phi_{ya} = (\partial\phi(x,y)/\partial y)_a$ ,  $\phi_{xb} = (\partial\phi(x,y)/\partial x)_b$ , and  $\phi_{yb} = (\partial\phi(x,y)/\partial y)_b$ . The term  $C_{j0}$  is the geometric matrix for the  $j^{\text{th}}$  member;  $\Phi_i$  is the  $j^{\text{th}}$  modal vector at the  $j^{\text{th}}$  member which connects two nodes  $a$  and  $b$ ; and  $l$  is the length of the  $j^{\text{th}}$  member.

Since only displacements in the z-direction were measured (e.g., as shown in Figs. 5-7), four rotational degrees of freedom in Eq. 14 had to be obtained by other means. First, the displacement in the z-direction (i.e., a modal vector of 36 degrees of freedom) was normalized. Next, a two dimensional interpolation was performed for the entire surface and rotations based on the interpolated mode shapes were obtained via numerical differentiation. Note that for each element of the grid model, the damage localization index given by Eq. 11 does not require to estimate either geometric quantities (e.g., the cross-sectional area or the second moment of area) or material properties (e.g., Young's modulus) of the structure.

### 3.4 Damage Localization in the Test Structure

For each level of damage, we performed the



damage localization in the test structure in four steps. In Step One, as the modal data to the grid model shown in Eq. 14, we selected three modes (which are out-of-plane flexural modes) shown in Figs. 5-7. In Step Two, the damage localization index given by Eq. 11 was computed for each damage stage. In Step Three, the criterion for the damage localization indicator (given by Eq. 13) was established as follows: (1) select  $H_0$  if  $Z_i < 2$  (i.e., no damage exists at member  $i$ ) and (2) select the alternate  $H_1$  if  $Z_i \geq 2$ . This criterion corresponds to a one-tailed test at a significance level of 0.024 (i.e., a probability of occurrence of 97.6 percent). In Step Four, this criterion was used to select potential damage locations in the test structure. The damage localization results for the two damage stages are shown in Fig. 9. Note that the true damage location in the test structure (i.e., fatigue crack location shown in Fig. 3) is corresponding to Element 30 in the damage detection model (shown in Fig. 8).

The following observations are made from Fig. 9. For Damage Stage One, damage is indicated at Elements 12, 13, and 30. For Damage Stage Two, damage is indicated at Elements 4, 5, 12, 13, and 30. For both cases, damage is predicted at or near to the correct location Element 30. Note that Elements 4, 5, 12, and 13 are adjacent to the correct location Element 30. From these results, we conclude that the proposed algorithm can localize damage in the reinforced concrete deck for which pre-damage and post-damage modal parameters are available for three flexural modes.

#### 4. SUMMARY AND CONCLUSIONS

The objective of this paper was to present a practical methodology to detect the location of damage in reinforced concrete structures for

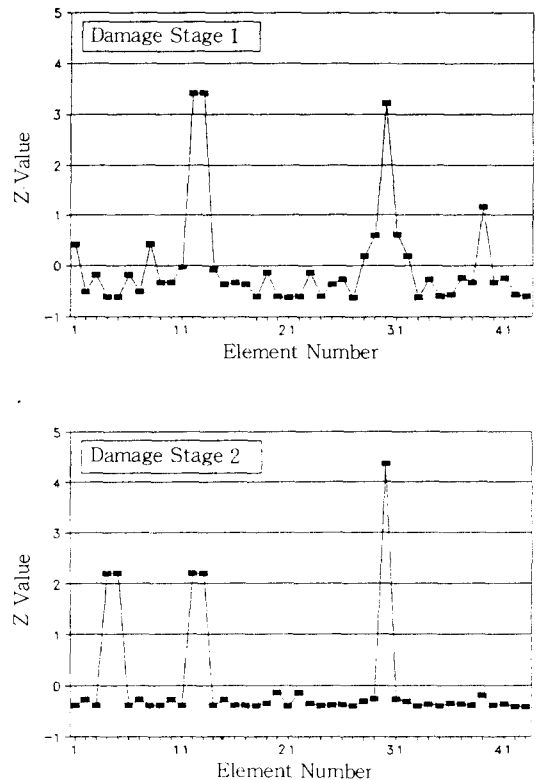


Fig. 9 Damage localization results for two damage stages

which as-built and post-damage modal parameters are available for few vibrational modes. This objective was met by performing two major parts. In the first part, we formulated an algorithm to localize damage directly from changes in mode shapes of structures. In the second part, we demonstrated that the proposed algorithm could detect and localize damage in a real, reinforced concrete structure for which mode shapes of three modes are available for both as-built and post-damage states.

From the material presented here, we conclude that it is possible to localize damage in a reinforced concrete structure with pre-damage and post-damage mode shapes of very few vibrational modes (in this study, three modes). Research to improve the damage detection al-

gorithm presented here is continuing along three lines of inquires. Firstly, we are developing algorithms to estimate the size of damage. Secondly, we are extending the algorithm to more complicated structures such as three dimensional frames. Thirdly, we are now in advanced stages of demonstrating the practicality of the approach in damage localization and severity estimation in full-scale structures.

## REFERENCES

1. Biswas, M., Pandey, A.K., and Samman, M. M. (1990). "Modal Technology for Damage Detection of Bridges", NATO Workshop on Bridge Evaluation, Repair and Rehabilitation, ed. A. Nowak, Kluwer Academic Publishers, Maryland, pp.161-174.
2. Cawley, P., and Adams, R.D. (1979). "The Location of Defects in Structures from Measurements of Natural Frequencies", J. Strain Analysis, Vol. 14, No. 2, pp.49-57.
3. Chen, J., and Garba, J.A. (1988). "On-Orbit Damage Assessment for Large Space Structures", AIAA Journal, Vol. 26, No. 9, pp. 1119-1126.
4. Chondros, T.G., and Dimarogonas, A.D. (1980). "Identification of Cracks in Welded Joints of Complex Structures", J. Sound and Vibration, Vol. 69, No. 4, pp.531-538.
5. Crohas, H., and Lepert, P. (1982). "Damage-Detection Monitoring Method for Offshore Platforms is Field-Tested", Oil and Gas J., pp.94-103.
6. Egger, D.W., and Stubbs, N. (1993). "Structural Assessment using Modal Analysis Techniques", IMAC '93, Honolulu, Hawaii.
7. Fletch, R.G., and Kernichler, K. (1990). "A Dynamic Method for the Safety Inspection of Large Prestressed Bridges", NATO Workshop on Bridge Evaluation, Repair and Rehabilitation, ed. A. Nowak, Kluwer Academic Publishers, Maryland, pp.175-186.
8. Gibson, J.D., and Melsa, J.L. (1975). "Introduction to Nonparametric Detection with Applications", Academic Press, New York.
9. Gudmunson, P. (1982). "Eigenfrequency Changes of Structures Due to Cracks, Notches or Other Geometrical Changes", J. Mech. Phys. Solids, Vol. 30, No. 5, pp.339-353.
10. Kenley, R.M., and Dodds, C.J. (1980). "West Sole WE Platform: Detection of Damage by Structural Response Measurements", Off-shore Tech. Conf., Houston, pp.111-118.
11. Kim, J.T., and Stubbs, N. (1994). "Damage Detection in Jacket-Type Offshore Structures From Few Mode Shapes", Journal of Ocean Engineering and Technology of Korea, Vol. 8, No. 1, pp.144-153.
12. Kosko, B. (1992). "Neural Networks for Signal Processing", Prentice Hall, New Jersey.
13. Mazurek, D.F., and DeWolf, J.T. (1990). "Experimental Study of Bridge Monitoring Technique", J. of Structural Engineering, ASCE, Vol. 116, No. 9, pp.2532-2549.
14. Nielson, R.O. (1991). "Sonar Signal Processing", Artech House, London.
15. O'Brien, T.K. (1980). "Stiffness Change As A Nondestructive Damage Measurement, Mechanics of Non-destructive Testing", ed. W.W. Stinchcomb, Plenum Press, USA
16. Star Reference Manual. (1990). Structural Measurement Systems, Inc., California, USA.
17. Stubbs, N., and Osegueda, R. (1990). "Global Non-Destructive Damage Evaluation in Solids", Int. J. Anal. Exp. Modal Analysis, Vol. 5, No. 2, pp.67-79.
18. Stubbs, N., Kim, J.T., and Topole, K.G., (1992) "An Efficient and Robust Algorithm for Damage Localization in Offshore Platforms", Tenth Structural Congress '92, ASCE, San Antonio, Texas, April 13-15, pp.543-546.
19. Stubbs, N., Kim, J.T., and Topole, K.G. (1993). "Experimental Determination of System Stochasticity", Structural Safety and Reliability, Proceedings of ICOSSAR'93, Innsbruck, Austria, pp.369-374.
20. Ugural, A.C. (1981). Stress in Plates and Shells, McGraw-Hill, New York, USA

(접수일자 : 1994. 10. 17)